

1 Estimation of in-canopy ammonia sources and sinks in a fertilized

2 *Zea mays* field

3
4 Jesse O. Bash¹, John T. Walker², Gabriel G. Katul³, Matthew R. Jones², Eiko Nemitz⁴,

5 Wayne P. Robarge⁵

6 1. National Exposure Research Laboratory, U.S. Environmental Protection Agency, Research
7 Triangle Park, NC, 27711, United States

8 2. National Risk Management Research Laboratory, U.S. Environmental Protection Agency,
9 Research Triangle Park, NC, 27711, United States

10 3. Nicholas School of the Environment, Duke University, Durham, NC 27708-0328, United States

11 4. Centre for Ecology and Hydrology (CEH) Edinburgh, Bush Estate, Penicuik, EH26 0QB, United
12 Kingdom.

13 5. Department of Soil Science, North Carolina State University, Raleigh, NC, 27695, United States

Abstract:

An analytical model was developed to describe in-canopy vertical distribution of ammonia (NH_3) sources and sinks and vertical fluxes in a fertilized agricultural setting using measured in-canopy mean NH_3 concentration and wind speed profiles. This model was applied to quantify in-canopy air-surface exchange rates and above-canopy NH_3 fluxes in a fertilized corn (*Zea Mays*) field. Modeled air-canopy NH_3 fluxes agreed well with independent above-canopy flux estimates. Based on the model results, the urea fertilized soil surface was a consistent source of NH_3 one month following the fertilizer application, while the vegetation canopy was typically a net NH_3 sink with the lower portion of the canopy being a constant sink. The model results suggested that the canopy was a sink for some 70% of the estimated soil NH_3 emissions. A logical conclusion is that parameterization of within-canopy processes in air quality models are necessary to explore the impact of agricultural field level management practices on regional air quality. Moreover, there are agronomic and environmental benefits to timing liquid fertilizer applications as close to canopy closure as possible. Finally, given the large within-canopy mean NH_3 concentration gradients in such agricultural setting, a discussion about the suitability of the proposed model is also presented.

1. Introduction

Over the past three decades, interest in measuring and modeling bidirectional exchanges of NH_3 between the biosphere and the atmosphere has proliferated for a number of reasons. NH_3 plays a primary role in aerosol formation because it is an atmospheric acid-neutralizing agent. Atmospheric ammonium nitrate and ammonium

sulfate aerosol adversely influences human health (1), decreases visibility, and affects atmospheric radiative forcing (2). NH_3 deposition also adversely affect ecosystems by contributing to soil acidification and habitat loss related to excess nutrient loading (3). Biological processes in soils enriched by reduced nitrogen (NH_x) deposition can lead to emissions of NH_3 and nitrous oxide, a greenhouse gas (3), and vegetation can act as a sink or source of atmospheric NH_3 (4). The use of NH_x as a fertilizer in agricultural processes has dramatically increased over the past century and the trend is expected to continue with an increasing demand for biofuels and to simply meet the nutritional requirements of an increasing global population (5).

The impact of human activity on the nitrogen cycle has made the parameterization of NH_3 emissions and deposition in air quality models an active area of research for determining sound regulatory scenarios for human exposure to particulates, ecosystem nutrient loading and climate change (2). The largest sources of atmospheric NH_3 are large-scale livestock operations and fertilized agricultural fields (3). Recent research has led to the development of mechanistic models to describe emissions from livestock operations (6) and air-vegetation NH_3 exchange (7). However, the role of vegetation in regulating NH_3 emissions from fertilized agricultural fields remains a subject of research (8) that lacks analytical tractability and a clear organizing framework for evaluating field measurements.

A process level understanding of biological, chemical and mechanical processes influencing the soil-vegetation-atmosphere exchange of nitrogen over a variety of managed and natural ecosystems remains needed before the impact of field scale mitigation strategies on regional air quality can be realized (9). Progress has recently

1 been made in elucidating the mechanisms driving NH_3 air-surface exchange.
2 Bidirectional NH_3 exchange models that include stomatal compensation points, the
3 equilibrium surface concentration when there is no net exchange, and parameterization of
4 dynamic leaf surface chemistry models have been developed (7,10-12) and adapted in a
5 number of applications (13). Also, a process-based understanding of NH_3 exchange
6 across atmospheric-stomatal cavity and atmospheric-vegetation surface interfaces has
7 been proposed (8). Nevertheless, the effect of soil emission processes and alteration of in-
8 canopy sources and sinks by enriched NH_3 concentration in these deeper layers of the
9 canopy remain vexing research problems to be confronted (2).

10 Above-canopy NH_3 fluxes can be estimated using micrometeorological
11 techniques, flux gradient approaches (6,14), relaxed eddy accumulation (15,16), or
12 directly measured via eddy covariance methods (17). Such measurements are a net soil-
13 canopy-atmosphere flux and do not distinguish between soil and vegetation contributions
14 needed to advance model development (2). In-canopy sources and sinks of NH_3 enriched
15 in a stable isotope of nitrogen have been made by using flux chambers (12), though the
16 small scale of such measurements are 'cursed' by large spatial variability.

17 Canopy-scale sources, sinks, and fluxes may be inferred based on an 'inversion'
18 using in-canopy mean scalar concentration profile measurements (18-21). Two broad
19 'inversion' approaches exist; Eulerian-based closure schemes that vary in complexity
20 (e.g. 22-28) and Lagrangian near field (LNF) dispersion models (23, 29-30). Higher
21 order Eulerian methods generally require measurements or modeling of the in-canopy
22 flow field, but more important, they require the turbulent kinetic energy dissipation rate
23 or the relaxation time scale profiles. These quantities are notoriously difficult to model or

1 measure inside dense canopies. Likewise, LNF requires knowledge of vertical
2 distributions of Lagrangian time scales and vertical velocity standard deviation.
3 Uncertainties in these parameters can lead to unrealistic integrated flux profiles (19,31).
4 To date, a simplified analytical method that can explicitly predict canopy sources and
5 fluxes of NH_3 from mean concentration profiles is desirable but lacking, though interest
6 in this topic is gaining popularity in canopy turbulence research (32).

7 Here, we propose a simplified analytical model that describes the in-canopy
8 vertical distribution of NH_3 sources and sinks and vertical fluxes in a fertilized
9 agricultural setting aimed at quantifying in-canopy air-surface exchange and above-
10 canopy NH_3 flux. While simplified analytical models can be criticized ‘ad-infinity’,
11 especially when they are theoretically anchored to first-order closure principles, the
12 technique proposed here provides constraints that allow above-canopy fluxes, soil and
13 leaf chemistry measurements, and measurements of environmental variables to be
14 interpreted. The fact that this approach is applied to a fertilized agricultural setting often
15 characterized by large mean vertical gradients in NH_3 concentrations permits some
16 theoretical justification for the usage of first-order closure principles. Performance of the
17 model was also evaluated against direct eddy covariance measurements of sensible heat
18 fluxes and modified Bowen ratio (MBR) fluxes of above canopy NH_3 fluxes collected at
19 the field site.

20 21 **2. Experimental Section**

22 **2.1 Site description**

1 The site was a 200 ha agricultural field near Lillington, North Carolina (35° 22'
2 35.7" Lat. -78° 46' 45.1" Long. 45 m Elev.). Soils were primarily fine sandy loam
3 (Exum series) with a texture of 21%, 68%, and 11% sand, silt, and clay, respectively.
4 Beneath the canopy, the ground surface was primarily exposed soil with little leaf litter or
5 organic matter. The field was planted in corn (*Zea mays*, Pioneer varieties 31G66 and
6 31P41, density of ≈ 70000 plants ha⁻¹) and fertilized with 50 kg N ha⁻¹ ammonium
7 polyphosphate (injected) between 4/18/07 and 4/23/07. The field was fertilized again
8 between 5/25/07 and 5/29/07 with 135 kg N ha⁻¹ urea ammonium nitrate solution (surface
9 applied) containing Agrotain[®] nitrogen stabilizer. The canopy reached a peak leaf area
10 index (single-sided) of 2.9 ± 0.6 m² m⁻² and a maximum canopy height (h_c) of 2.2 m near
11 7/15/07 and had fully senesced by 8/21/07.

13 2.2 In-canopy measurements

14 In-canopy mean velocity, air temperature and NH₃ concentration profiles were
15 measured from July 6th through August 1st, 2007. An ATI 3D sonic anemometer (Applied
16 Technologies, Inc., Longmont, CO, U.S.A) was mounted on an adjustable bracket to
17 measure sensible heat and momentum fluxes within the canopy. The sonic anemometer
18 was sampled at 10 Hz and mounted from 0.5 to 1.5 m above the soil surface. In-canopy
19 NH₃ concentrations were measured using duplicate phosphorous acid coated annular
20 denuders (URG, Chapel Hill, NC, U.S.A.) mounted at 0.1, 0.3, 0.95, 1.5, and 2.25 m
21 above ground level. Denuders were sampled for approximately two hours each at an air
22 flow rate of 20 L min⁻¹. After sampling, denuders were extracted with 2.5 mL deionized
23 water and analyzed for NH₄⁺ by ion chromatography (Model DX120, Dionex

Corporation, Sunnyvale, CA, U.S.A.). Air concentrations ($\mu\text{g NH}_3 \text{ m}^{-3}$) were calculated by dividing the mass of NH_3 collected by the total volume of air sampled. Excellent precision was achieved between paired in-canopy denuder replicates; the median relative difference was 4.6% ($N = 45$). Each denuder set was collocated with a copper-constantan thermocouple sampled at a frequency of 1 Hz. Leaf temperatures were sampled at 1 Hz using copper-constantan thermocouples affixed to the leaf surfaces at 0.65, 0.85, 1.4, 1.8, and 1.8 m above the ground level. Apoplastic $[\text{NH}_4^+]$ and pH were measured from extracted leaf apoplastic solution by using the vacuum infiltration technique (33) to directly measure the canopy's emission potential.

2.3 Above-canopy measurements

R.M. Young Model 81000 sonic anemometers (R.M Young Company, Traverse City, MI, USA) were mounted at 2.5, 3.5 and 10 m above the ground level and a leaf wetness sensor was mounted at the canopy height (Campbell Scientific, Model 237, Logan, UT). Four collocated phosphorous acid coated denuders (URG, Chapel Hill, NC, U.S.A.) mounted at 4.92 m above the soil surface were sampled for twelve hours each at an air flow rate of 10 L min^{-1} . Vertical NH_3 concentration gradients above the canopy were measured at 0.3 m and 2.4 m above the canopy with a continuous flow wet denuder system "AMANDA" (Ammonia Measurement by ANnular Denuder sampling with online Analysis; 14). Gaseous NH_3 was collected from the sample airstream (30 L min^{-1}) in a wetted continuous-flow annular denuder using a stripping solution of 3.6 mM NaHSO_4 . The aqueous NH_3 concentration was determined by a detector based on a selective ion membrane and online conductivity analysis (detection limit $\approx 0.02 \mu\text{g NH}_3$

m⁻³) by sequentially sampling each denuder such that a vertical profile was determined every 15 minutes for 30 minute flux calculations. Copper-constantan thermocouples were collocated with annular denuders to measure ambient mean air temperature profiles.

2.4 Modified Bowen ratio for above-canopy fluxes

Above-canopy NH₃ fluxes were estimated using the modified Bowen ratio (MBR) method. The MBR method assumes the turbulent diffusivity of NH₃ is similar to the turbulent diffusivity of heat such that

$$F_{NH_3} = \overline{w'T'} \frac{\Delta \overline{C}}{\Delta \overline{T}} = \overline{w'T'} \frac{\overline{C}(z_1) - \overline{C}(z_2)}{\overline{T}(z_1) - \overline{T}(z_2)}, \quad (1)$$

where F_{NH_3} is the air-canopy flux of NH₃, $\overline{w'T'}$ the eddy-covariance measured sensible heat flux and, $\Delta \overline{C}$ and $\Delta \overline{T}$ are co-located mean NH₃ concentration and air temperature measured differences at heights z_1 and z_2 .

2.5 Analytical first-order closure model for in-canopy fluxes

The mean in-canopy continuity equation for a stationary and planar-homogeneous high Reynolds number flow in the absence of subsidence can be expressed as

$$\frac{\partial \overline{C}}{\partial t} = -\frac{\partial \overline{w'C'}}{\partial z} - S(z) = 0, \quad (2)$$

where C is a scalar concentration (e.g. NH₃), $\overline{w'C'}$ is the scalar flux and $S(z)$ is the source/sink rate of C . The scalar flux can be estimated using gradient-diffusion (K) theory;

$$\overline{w'C'} = -K_e \frac{\partial \overline{C}}{\partial z}, \quad (3)$$

where K_e is the eddy diffusivity for NH_3 . While first order closure models are often questionable inside canopies (29), this approximation may be valid for NH_3 under conditions associated with fertilized cropping systems where NH_3 concentration profiles would be expected to decrease monotonically with height (Text S1). In-canopy eddy diffusivity can be characterized from the mean wind speed profile and the mixing length hypothesis via

$$K_e = \frac{1}{\text{Pr}} L_m^2 \left| \frac{\partial \overline{U}}{\partial z} \right|, \quad (4)$$

where L_m is the mixing length, and Pr is the turbulent Prandtl number (34). Pr is near unity for near-neutral flows in the atmospheric surface layer (ASL); however, values as low as 0.5 have been reported near the canopy top (35).

The mixing length is parameterized following Harman and Finnigan (34):

$$L_m = \frac{2\beta^3}{C_d a(z) \varphi_m \left(\frac{h_c - d}{L} \right)}, \quad (5)$$

where β is the dimensionless momentum flux $\left(u_* / \overline{U} \Big|_{z=h_c} \right)$, C_d is the product of the in-canopy drag coefficient and the sheltering factor (typically between 0.1 and 0.3: 36), a is the mean leaf area density, the ratio of the plant area index to the canopy height (h_c), d is

1 the zero plane displacement, L is the Obukhov length, and ϕ_m is the dimensionless
 2 correction factor for atmospheric stability.

3 The in-canopy mean wind speed profile, turbulent diffusivity for momentum
 4 ($K_t = K_e \text{Pr}$), and momentum flux ($\overline{u'w'}$) are based on the analytical solution of Inoue
 5 (37) following the parameterization of Harman and Finnigan (34):

$$\begin{aligned} \overline{U}(z) &= \overline{U}(h_c) \exp \left[\frac{\beta(z-h_c)}{L_m} \right] \Big|_{z < h_c} \\ 6 \quad K_t &= \beta L_m \overline{U}(z) \quad , \\ \overline{u'w'} &= -(\beta \overline{U}(z))^2 \end{aligned} \quad (6)$$

7 The above-canopy stability corrected log-linear mean wind speed profile was used to
 8 scale the wind speed measured at 2.5 and 3.5 m to the canopy height ($z = h_c$) following
 9 Byun (38)

$$10 \quad \overline{U}(z) = \frac{u_*}{k} \left(\ln \left[\frac{z-d}{z_o} \right] + \psi \left(\frac{z-d}{L} \right) - \psi \left(\frac{z_o}{L} \right) \right) \Big|_{z/h_c > 1} \quad , \quad (7)$$

11 where z_o is the momentum roughness length, d is the zero plane displacement ($0.1 h_c$ and
 12 $2/3 h_c$ respectively), $k = 0.4$ is von Karman's constant, and ψ is the integrated diabatic
 13 stability correction.

14 Upon substituting these approximations into equation (2), the NH_3 sources and
 15 sinks are now analytically linked to the measured mean concentration profile, momentum

1 absorption by the canopy drag elements, mixing length, and the friction velocity at the
2 canopy top via

$$3 \quad S(z) = \begin{cases} -\frac{u_*}{Pr} \exp\left[\beta\left(\frac{z-h_c}{L}\right)\right] \left(L_m \frac{\partial^2 \bar{C}}{\partial z^2} + \beta \frac{\partial \bar{C}}{\partial z}\right); & z/h_c \leq 1, \\ 0; & z/h_c > 1 \end{cases}, \quad (8)$$

4 The turbulent fluxes can be inferred by integrating equation (2) after solving equation (8)
5 using measured mean concentration profiles.

6

7 **3. Results and Discussion**

8 **3.1 Wind profiles**

9 Because the vertical variation of the momentum eddy diffusivity is central to the
10 description of $S(z)$, the analytical model for mean velocity and turbulent stress was
11 compared to the Wilson (39) data for a similarly structured corn canopy ($LAI = 2.9$, $h_c =$
12 2.21 m) corn canopy (Figure 1). For reference, K- ϵ model results described in Katul *et al.*
13 (36) are also shown in Figure 1. Both the analytical and K- ϵ models captured the
14 variations well in wind speed profiles measured by Wilson (39), with coefficient of
15 determination (r^2) values of 0.987 and 0.989, respectively. When the analytical model
16 was applied to field data, a clear underestimation in the measured in-canopy wind speed
17 profiles under stable conditions emerged using the *a priori* specified drag coefficient
18 ($C_d=0.3$) of Wilson (39).

The best estimate of the wind profile over a variety of stability regimes was found when the in-canopy drag coefficient was solved from the parameterization of the in-canopy momentum flux, Equations 5 and 6, and measured momentum fluxes. The parameterization of a vertically invariant in-canopy drag coefficient is reasonable for a corn canopy, known to have a relatively uniform vertical distribution of leaf area densities and closed understory. However if this formulation is to be applied for a canopy with an open understory and more variable leaf area density, the drag coefficient should be parameterized as a function of height (40-41).

3.2 Turbulent sensible heat flux estimation

Sensible heat fluxes estimated by integrating the source-sink profile of the analytical closure model from the soil surface ($z=0$) up to the canopy height ($z=h_c$) correlate well with measured sensible heat fluxes. Comparison of above-canopy fluxes by regression analysis indicates a linear relationship with a slope of 1.05 and intercept of $-8.30 \times 10^{-3} \text{ } ^\circ\text{C m s}^{-1}$ ($r^2 = 0.854$, $p < 0.001$, $N = 341$); mean normalized bias and error are -21% and 50%, respectively. Comparison of in-canopy measured and modeled fluxes yields a slope of 0.646 and intercept of $-1.72 \times 10^{-3} \text{ } ^\circ\text{C m s}^{-1}$ ($r^2 = 0.632$, $p < 0.001$, $N = 341$) with mean normalized bias and error of -49% and 59%, respectively (Figure 2). Above-canopy sensible heat fluxes were underestimated during the morning transition when the upper canopy was being heated and overestimated during the evening transition when the upper canopy was cooling (when stationarity assumptions are questionable). In-canopy sensible heat fluxes were underestimated during the mid-day peak, possibly because the model does not consider soil heat storage (see Text S1).

1 It is important to note that, while the sensible heat flux is commonly used to
2 evaluate in-canopy source/sink models, in this case such a comparison may represent a
3 worst case test of the model. The first-order approach presented here should perform best
4 when a large monotonic gradient is present. As described in Supplemental Material
5 sections S1 and S2, the measured NH_3 concentration gradients are always much larger
6 than the corresponding temperature gradients. While the agreement between measured
7 and modeled heat fluxes presented here is comparable to and in some cases exceeds the
8 performance of other Eulerian and LNF techniques (22-30) in different canopies, it may
9 not be truly indicative of the skill of the proposed method. Comparison to the flux of a
10 non-reactive compound such as N_2O , which is emitted only from the soil and at similar
11 rates to NH_3 , would be more appropriate.

13 **3.3 Air-canopy ammonia flux estimates**

14 Measured in-canopy NH_3 concentration profiles were consistently near monotonic
15 during all in-canopy sampling periods with the magnitude of the concentration decreasing
16 with height from the soil surface to the top of the canopy suggesting that first-order
17 closure principles may be applicable (Text S1, Figure 3). In-canopy concentration
18 profiles were separated into three categories; (1) included samples that were taken
19 before sunrise when the atmosphere was typically stable (Figure 3a), (2) included
20 samples that were taken in mid to late morning during the canopy drying period (Figure
21 3b) and (3) included samples that were taken from late morning into the afternoon when
22 the canopy was typically dry and conditions were unstable (Figure 3c). Air-canopy scale
23 NH_3 fluxes estimated by integrating modeled in-canopy source sink profiles from the soil

1 surface to the canopy height compared well (regression slope = 0.882, significant at $p <$
2 0.001 and the intercept was not statistically different from 0) with above canopy MBR
3 flux measurements (Figure 4). When the largest evasive flux measured on July 6th was
4 removed from the analysis the slope dropped to 0.386 but the correlation was still
5 significant at $p < 0.05$ and the least squares regression line falls within the 95%
6 confidence interval, based on the variability of the flux in each sampling period, of 6 of
7 the remaining 8 sets of MBR flux measurements.

9 **3.4 In-canopy NH₃ sources and sinks**

10 In-canopy source/sink and concentration profiles indicate that, approximately one
11 month following fertilizer application, the canopy recaptures the majority NH₃ emitted
12 from the soil surface. On average, 73% of soil NH₃ emissions were taken up by the
13 canopy at a mean rate of $118 \text{ ng m}^{-2} \text{ s}^{-1}$. Canopy uptake was similar in magnitude to the
14 sugar cane crop studied by Denmead *et al* (18); however, the fractional uptake of
15 estimated soil emissions was much greater for this site. Soil emissions estimates and
16 mean concentration measurements of Denmead *et al.* (18) were one to two orders of
17 magnitude higher than presented here. The difference in the uptake of soil emissions may
18 be influenced by differences in the in-canopy ambient NH₃ concentrations and
19 fertilization rates, which drive the stomatal component of the foliage exchange through
20 the regulation of apoplast chemistry and, subsequently, the stomatal compensation point.

21 Net canopy compensation points, which represent the combined effects of
22 cuticular and stomatal exchange, were approximated by inverting the modeled source
23 sink profiles. This inversion is analogous to the technique applied to the LNF modeled

sources and sinks of Harper *et al.* (42). Upper canopy (i.e. $0.5 < z/h_c \leq 1$) modeled compensation point compared well with experimentally derived stomatal compensation points estimated from measured leaf temperature and apoplast NH_4^+ and H^+ concentrations (mean of $2.31 \mu\text{g m}^{-3}$ and $2.13 \mu\text{g m}^{-3}$ respectively). Exchange in the upper canopy was also bidirectional depending on the strength of the soil emissions, above canopy concentrations, and environmental parameters (e.g. leaf wetness, leaf temperature, relative humidity, *etc.*). This result is in good agreement with above canopy MBR measurements of Nemitz *et al.* (15) despite differences in the ground surface emissions sources (Table 1). Ground surface emissions were from fertilizer application here and from senescent leaves in the Nemitz *et al.* (15). Deeper in the canopy ($0 < z/h_c < 0.5$), the sinks remain persistent through daytime and early morning hours when stomatal exchange is expected to be small suggesting that cuticular processes dominate uptake in these lower canopy layers, while the stomatal component of the net air-surface exchange is relatively more important in the upper canopy layers. Modeled canopy compensation points were approximately half of the values for *Z. mays* reported by Harper and Sharpe (21) and at least an order of magnitude lower than those estimated by Harper *et al.* (42) using the LNF dispersion technique, although these studies also reported ambient concentrations at least an order of magnitude larger than those measured here.

In-canopy source/sink estimates for stable night-time conditions indicate a net NH_3 deposition to the canopy, in agreement with above-canopy MBR fluxes. In-canopy concentrations increased through early morning sampling, during stable periods, peaking at approximately 9:30 AM and then decreasing during late morning and afternoon hours

presumably through venting of the canopy (Figure 3; Text S2). This observation is consistent with the observations of Nemitz et al. (19) in an oilseed rape (*Brassica napus*) canopy, where ground surface emissions from decomposing senesced leaves escaped the canopy only during windy night-time conditions.

A diel morning peak in above canopy ambient NH_3 concentrations and evasive MBR flux measurements, beginning at approximately 7:00 AM EST to a mean daily maximum at approximately 8:00 AM EST, was persistent during the month of in-canopy sampling (Figure 5). Leaf drying experiments were conducted to investigate if the morning 'spike' in mean NH_3 concentrations was, in part, due to the evasion of ammonium contained in dew droplets as the canopy dried. The average concentration of NH_4^+ in the leaf surface droplets was $689 \mu\text{g L}^{-1}$ (and ranged from 11 to $2989 \mu\text{g L}^{-1}$). During the leaf drying experiments, we measured $25 - 35 \text{ g H}_2\text{O m}^{-2}$ leaf area in the upper and middle canopy (with widely varying but smaller amounts in the lower canopy). Assuming a leaf area of $3.0 \text{ m}^2 \text{ m}^{-2}$ and further assuming that the canopy dries completely between sunrise and 9:30 AM (based on our measurements), an average emission flux $4.0 \text{ ng NH}_3 \text{ m}^2 \text{ s}^{-1}$ was calculated for the drying period. Using the maximum observed NH_4^+ concentration in dew water yields an estimated maximum emission during the drying of the canopy of $17.6 \text{ ng NH}_3 \text{ m}^2 \text{ s}^{-1}$, 5% to 21% of the median MBR flux of $84.7 \text{ ng NH}_3 \text{ m}^2 \text{ s}^{-1}$ measured for between 7 AM to 10 AM EST from July 6th through August 1st. The direction of the NH_3 flux estimation and concentration of NH_4^+ in the dew indicate that the peak in the morning NH_3 concentrations originated primarily from canopy and soil sources rather than dew as observed by Sutton *et al.* (10).

Closure model estimates of the evasion of NH_3 from the soil surface were assumed to be equal to the source/sink estimate at $z = 0$. This estimate is independent of soil physical and chemical processes and is based on the near soil surface concentration profile and model estimated eddy diffusivity constrained by the in-canopy measurements extrapolated to the soil surface using the first order closure model. Results indicate that the large in-canopy concentration gradient was driven by persistent emissions from the urea fertilized soil surface throughout the measurement period, Table 1, Figure S3. Soil surface emission and canopy uptake estimates were enhanced by rainfall (43) in agreement with Roelle and Aneja (44). Accumulation of NH_3 on vegetative surfaces have been shown to reduce canopy uptake (17,45) and enhanced uptake of NH_3 following precipitation may be due to wash-off. However, air motion and transport processes remain uncertain near the soil surface because, as in other in-canopy studies, measurements were not made near the soil surface ($z < 0.5$ m) due to the 0.1 m path length and sampling frequency of the sonic anemometer (19). The structure of the boundary layer near the soil surface is unresolved and typically ignored due to difficulties in measuring wind and scalar variables (46) at appropriate spatial and temporal scales. Estimates of the in canopy air-soil flux from the closure model include uncertainty in the extrapolation of the in-canopy exchange parameterizations to the soil surface. However, these uncertainties are also present for LNF and more complex Eulerian closure models and the presence of a strong near-monotonic measured concentration profile indicate that the soil was a local source of NH_3 emissions.

3.5 Field and regional scale applications

1 On average 26.8% of the emissions from the ground level were estimated to be
2 released to the atmosphere. Thus, there are agronomic and environmental benefits to
3 timing liquid fertilizer applications as close to canopy closure as possible while
4 considering the physiological nitrogen requirements of the crop (47-48).

5 The use of an analytical in-canopy source/sink model is useful in applying constraints
6 to the relative contributions of vegetation and soil to net canopy-scale fluxes of NH_3 . This
7 closure technique is more constrained by measurements than *a priori* specified empirical
8 resistances to partition above canopy fluxes into contributions from canopy and soil
9 sources. This simple model lacks the sophistication of higher order Eulerian closure and
10 LNF models but estimated canopy and soil sources and sinks agree reasonably well when
11 a strong monotonic in-canopy concentration profile is present. Furthermore, the model
12 presented here may be used to define in-canopy resistances and to constrain canopy and
13 soil NH_3 partitioning suitable for air-quality model air surface exchange algorithms. As
14 expected, model performance was poorest when there were weak non-monotonic scalar
15 concentration profiles within the canopy (Discussed in Text S1), particularly during
16 morning and evening transition periods when flow is non-stationary. The results obtained
17 using this technique are being used in conjunction with measurements of soil, apoplast
18 and vegetation surface chemistry and canopy structural and physiological parameters to
19 refine the bidirectional NH_3 surface exchange model currently in development for the
20 Community Multiscale Air Quality (CMAQ) model (49).

21
22 **Disclaimer**

1 Although this work was reviewed by EPA and approved for publication, it may not
2 necessarily reflect official Agency policy. Mention of commercial products does not
3 constitute endorsement by the Agency.

5 **Acknowledgements**

6 G. Katul acknowledges support from the National Science Foundation (NSF-EAR 06-
7 35787, NSF-EAR-06-28432, and NSF-ATM-0724088), and the Binational Agricultural
8 Research and Development (BARD, Research Grant No. IS3861-06). This work was
9 funded by USDA CSREES Air Quality Program Grant # 35112 and U.S. EPA Office of
10 Research and Development.

12 **Supporting Information Available**

13 Additional information on the assumptions and applicability of the first order closure
14 model. This material is available free of charge via the internet at [hppt://pubs.acs.org](http://pubs.acs.org).

16 **References**

- 17
18 (1) Pope, C.A.; Dockery, D.W.: Health effects of fine particulate air pollution: Lines that
19 connect. *J. Air Waste Manage. Assoc.* **2006**, *56*, 709-742
- 20 (2) Sutton, M.A.; Nemitz, E.; Erisman, JW, Beier, C.; Bahl, K.B.; Cellier, P.; de Vries,
21 W.; Cotrufo, F.; Skiba, U.; Di Marco, C.; *et al.*; Challenges in quantifying biosphere-
22 atmosphere exchange of nitrogen species, *Environ. Pollut.* **2007**, *150*, 125-139

- 1 (3) Vitousek, P.M.; Aber, J.D.; Howarth, R.W.; Linkens, G.E.; Matson, P.A.; Schindler,
2 D.W., Schlesinger, W.H., Tilman, D.G.; Human alteration of the global nitrogen
3 cycle: sources and consequences. *Ecol. Appl.* **1997**, *7*(3), 737-750
- 4 (4) Sutton, M.A.; Asman, W.A.H.; Schjørring, J.K.; Dry deposition of reduced nitrogen,
5 *Tellus* **1994**, *46B*, 255-273
- 6 (5) Erisman, J.W.; Sutton, M.A.; Galloway, J.; Klimont, Z.; Winiwarter, W.; How a
7 century of ammonia synthesis changed the world, *Nature Geosci.* **2008**, *1*, 636-639
- 8 (6) Teye, F.K.; Hautala, M.; Adaption of an ammonia volatilization model for a naturally
9 ventilated dairy building, *Atmos. Environ.* **2008**, *42*, 4345-4354
- 10 (7) Sutton, M.A.; Schjørring, J.K.; Wyers, G.P.; Plant-atmosphere exchange of ammonia,
11 *Phil. Trans. R. Soc. Lond. A* **1995**, *351*, 261-278
- 12 (8) Massad, R.S.; Loubet, B.; Tuzet, A.; Cellier, P.; Relationship between ammonia
13 stomatal compensation point and nitrogen metabolism in arable crops: Current status
14 of knowledge and potential modeling approaches, *Environ. Pollut.* **2008**, *154*, 390-
15 403
- 16 (9) Holland, E.A.; Braswell, B.H.; Sulzman, J.; Lamarque, J-F.; Nitrogen deposition
17 onto the United States and Western Europe: synthesis of observations and models.
18 *Ecol. Appl.* **2005**, *15*(1), 38-57
- 19 (10) Sutton, M.A.; Burkhardt, J.K.; Guerin, D.; Nemitz, E.; Fowler, D.; Development of
20 resistance models to describe measurements of bi-directional ammonia surface
21 atmosphere exchange. *Atmos. Environ.* **1998**, *32*, 473-480

- 1 (11) Nemitz, E.; Milford, C.; Sutton, M.A.; A two-layer canopy compensation point
2 model for describing bi-directional biosphere-atmosphere exchange of ammonia. *Q.*
3 *J. R. Meteorol. Soc.* **2001**, *127*, 815-833
- 4 (12) Jones, M.R.; Raven, J.A.; Leith, I.D.; Cape, J.N.; Smith, R.I.; Fowler, D.; Short-term
5 flux chamber experiment to quantify the deposition of gaseous $^{15}\text{N-NH}_3$ to *Calluna*
6 *vulgaris*. *Agric. For. Meteorol.* **2008**, *148*(6-7), 893-901
- 7 (13) Walker, J.T.; Robarge, W.P.; Wu, Y.; Meyers, T.P.; Measurements of bi-directional
8 ammonia fluxes over soybean using the modified Bowen-ratio technique. *Agric. For.*
9 *Meteorol.* **2006**, *138*, 54-68
- 10 (14) Wyers, G.P.; Otyes, R.P.; Slanina, J.; A continuous-flow denuder for the
11 measurement of ambient concentrations and surface exchange of ammonia. *Atmos.*
12 *Environ.* **1993**, *27A*, 2085-2090
- 13 (15) Nemitz, E.; Flynn, M.; Williams, P.I.; Milford, C.; Theobald, M.R.; Blatter, A.;
14 Ballagher, M.W.; Sutton, M.A.; A relaxed eddy accumulation system for the
15 automated measurement of atmospheric ammonia fluxes. *Water Air Soil Poll.*, **2001**,
16 *1*(5-6), 189-202
- 17 (16) Hensen, A.; Nemitz, E.; Flynn, M.J.; Blatter, A.; Jones, S.K.; Sørensen, L.L.;
18 Hensen, B.; Pryor, S.; Jensen, B.; Otjes, R.P.; *et al.*; Sutton, M.A.; Inter-comparison
19 of ammonia fluxes obtained using the eddy accumulation technique. *Biogeosciences*
20 *Discuss.* **2008**, *5*, 3965-4000
- 21 (17) Whitehead, J. D.; Twigg, M.; Famulari, D.; Nemitz, E.; Sutton, M. A.; Gallagher, M.
22 W.; Fowler, D.; Evaluation of laser absorption spectroscopic techniques for eddy

covariance flux measurements of ammonia, *Environ. Sci. Technol.* **2008**, 42, 2041–2046.

(18) Denmead, O.T.; Freney, J.R.; Dunin, F.X.; Gas exchange between plant canopies and the atmosphere: case-studies for ammonia, *Atmos. Environ.* **2008**, 42, 3,394–3,406

(19) Nemitz E.; Sutton M.A.; Gut A.; San José R.; Husted S.; Schjørring J.K.; Sources and sinks of ammonia within an oilseed rape canopy. *Agric. Forest Meteorol.* **2000**, 105(4), 385-404

(20) Nemitz, E.; Loubet, B.; Lehmann, B.E.; Cellier, P.; Neftel, A.; Jones, S.K.; Hensen, A.; Ihly, B.; Tarakanov, S.V.; Sutton, M.A.; Turbulence characteristics in grassland canopies and implications for tracer transport. *Biogeosciences Discuss.* **2009**, 6, 437-489

(21) Harper, L.A.; Sharpe, R.R.; Nitrogen dynamics in irrigated corn – soil-plant nitrogen and atmospheric ammonia transport. *Agron. J.* **1995**, 87(4), 669-675

(22) Katul, G.G.; Albertson, J.D.; Modeling CO₂ sources, sinks, and fluxes within a forest canopy. *J. Geophys. Res.* **1999**, 104(D6), 6081-6091

(23) Siqueira, M.; Katul, G.G.; Lai, C-T.; Quantifying net ecosystem exchange by multilevel ecophysiological and turbulent transport models, *Adv. Water Resour.* **2002**, 25, 1357-1366

(24) Siqueira, M.; Lai, C-T.; Katul, G.G.; Estimating scalar sources, sinks and fluxes in a forest canopy using Lagrangian, Eulerian, and hybrid inverse models, *J. Geophys. Res.* **2000**, 105(D24), 29475-29488

- 1 (25) Siqueira, M.; Leuning, R.; Kolle, O.; Kelliher, F.M.; Katul, G.G.: Modelling sources
2 and sinks of CO₂, H₂O and heat within a Siberian pine forest using three inverse
3 methods, *Q. J. R. Meteorol. Soc.* **2003**, *129*(590), 1373-1393
- 4 (26) Siqueira, M.; Katul, G.G.; Estimating heat sources and fluxes in thermally stratified
5 canopy flows using higher-order closure models, *Boundary Layer Meteorol.* **2002**,
6 *103*, 125-142
- 7 (27) Cava, D.; Katul, G.G.; Scrimieri, A.; Poggi, D.; Cescatti, A.; Giostra, U.; Buoyancy
8 and the sensible heat flux budget within dense canopies, *Boundary Layer Meteorol.*
9 **2006**, *118*, 217-240
- 10 (28) Juang, J-Y.; Katul, G.G.; Siqueira, M.B.; Stoy, P.C.; Palmroth, S.; McCarthy, H. R.;
11 Kim, H.S.; Oren, R.; Modeling nighttime ecosystem respiration from measured CO₂
12 concentration and air temperature profiles using inverse methods, *J. Geophys. Res.*
13 **2006**, *111*, D08S05
- 14 (29) Raupach M.R.; A practical Lagrangian method for relating scalar concentrations to
15 source distributions in vegetation canopies. *Q. J. R. Meteorol. Soc.* **1989**, *115*, 609–32.
- 16 (30) Katul, G.G.; Oren, R.; Ellsworth, D.; Hsieh, C.I.; Phillips, N.; Lewin, K.; A
17 Lagrangian dispersion model for predicting CO₂ sources, sinks, and fluxes in a
18 uniform loblolly pine (*Pinus taeda L.*) stand. *J. Geophys. Res.* **1997**, *102*, 9309–9321.
- 19 (31) Leuning, R.; Denmead, O.T.; Miyata, A.; Kim, J.; Source/sink distributions of heat,
20 water vapour, carbon dioxide and methane in a rice canopy estimated using
21 Lagrangian dispersion analysis, *Agric. For. Meteorol.* **2000**, *104*, 233-249
- 22 (32) Harman, I.N.; Finnigan, J.J.; Scalar concentration profiles in the canopy and
23 roughness sublayer, *Boundary Layer Meteorol.* **2008**, *129*, 323-351

- 1 (33) Husted, S.; Schjoerring, J.K.; Ammonia flux between oilseed rape plants and the
2 atmosphere in response to changes in leaf temperature, light intensity, and air
3 humidity, *Plant Physiol.* **1996**, 112, 67-74
- 4 (34) Harman, I.N.; Finnigan, J.J.; A simple unified theory for flow in the canopy and
5 roughness sublayer, *Boundary Layer Meteorol.* **2007**, 123, 339-363
- 6 (35) Finnigan, J.; Turbulence in plant canopies, *Annu. Rev. Fluid Mech.* **2000**, 32, 519-
7 571
- 8 (36) Katul, G.G.; Mahrt, L.; Poggi, D.; Sanz, C.; One- and two-equation models for
9 canopy turbulence, *Boundary Layer Meteorol.* **2004**, 113, 81-109
- 10 (37) Inoue, E.; On the turbulent structure of air flow within crop canopies. *J. Meteorol.*
11 *Soc. Japan*, **1963**, 41, 317-326
- 12 (38) Byun, D.W.; On the analytical solution to the flux-profile relationships for the
13 atmospheric surface layer. *J. Appl. Meteor.* **1990**, 29, 652-657
- 14 (39) Wilson, J.D.; A 2nd order closure model for flow through vegetation. *Boundary-*
15 *Layer Meteorol.* **1988**, 42, 371-392
- 16 (40) Yi, C.; Momentum transfer within canopies, *J. Appl. Meteor. Clim.* **2008**, 47, 262-
17 275
- 18 (41) Poggi, D.; Porporato, A.; Ridolfi, L.; Albertson, J. D.; Katul, G.G.; The effect of
19 vegetation density on canopy sub-layer turbulence, *Boundary-Layer Meteorol.* **2004**,
20 111, 565-587.
- 21 (42) Harper, L.A.; Denmead, O.T.; Sharpe, R.R.; Identifying sources and sinks of scalars
22 in a corn canopy with inverse Lagrangian dispersion analysis II. Ammonia, *Agric.*
23 *For. Meteorol.* **2000**, 104, 75-83

- (43) Walker, J.T.; Jones, M.R.; Bash, J.O.; Myles, L.; Luke, W.; Meyers, T.P.; Robarge, W.; Air surface exchange of ammonia in a fertilized corn canopy from planting through senescence. *In preparation*
- (44) Roelle, P.A.; Aneja, V.P.; Characterization of ammonia emissions from soils in the upper coastal plain, North Carolina., *Atmos. Environ.* **2002**, *36*, 1087-1097
- (45) Jones, M.R.; Leith, I.D.; Fowler, D.; Raven, J.A.; Sutton, M.A.; Nemitz, E.; Cape, J.N.; Sheppard, L.J.; Smith, R.I.; Theobald, M.R.; Concentration-dependent NH_3 deposition processes for mixed moorland semi-natural vegetation. *Atmos. Environ.* **2007**, *41(10)*, 8980-8994
- (46) Wilson, J.D.; Flesch, T.K.; Flow boundaries in random-flight dispersion models: enforcing the well-mixed condition. *J. Appl. Meteorol.* **1993**, *32*, 1695-1707
- (47) Sommer, S.G.; Schjoerring, J.K.; Denmead, O.T.; Ammonia emissions from mineral fertilizers and fertilized crops. *Advanc. Agron.* **2004**, *82*, 557-622
- (48) Sommer, S.G.; Friis, E.; Bach, A.; Schjørring, J.K.; Ammonia volatilization from pig slurry applied with trail hoses or broadcast to winter wheat: effects of crop development stage, microclimate, and leaf ammonia absorption. *J. Environ. Qual.* **1997**, *26*, 1153-1160
- (49) Byun, D.; Schere, K.L.; Review of the governing equations, computational algorithms, and other components of the Models-3 Community Multiscale Air Quality (CMAQ) modeling system. *Appl. Mech. Rev.* **2006**, *59*, 51-77

Tables

Table 1. Canopy flux, uptake and compensation point estimates and meteorological conditions, where T_a is the mean ambient temperature at the canopy top, T_L is the mean leaf temperature, T_s is the mean soil temperature at $z = -5$ cm, RH is the relative humidity, and Γ is the leaf emission potential at the canopy height assuming the flux is stomatally controlled.

Date	Time	Soil Flux* ng m ⁻² s ⁻¹	Net Flux* ng m ⁻² s ⁻¹	Canopy Flux* ng m ⁻² s ⁻¹	$U(h_d)$ m/s	$u^*(h_d)$ m/s	h_d/L m/m	Canopy wetness % time	T_a °C	T_L °C	T_s °C	RH %	Comp point μg m ³	Γ $\frac{[NH_4^+]}{[H^+]}$
6-Jul ³	11:30-14:00	13.7	275	258	1.61	0.328	-0.255	0.0	31.68	34.76	29.46	48.35	7.43	370
9-Jul ³	9:35-12:45	185	39.6	-146	1.316	0.262	-0.333	0.0	31.04	37.11	28.62	55.56	0.95	40
11-Jul ³	9:20-14:15	308	-13.8	-322	2.764	0.54	-0.002	0.7	31.74	32.67	28.57	53.55	2.01	125
11-Jul ³	14:30-17:40	281	41.0	-240	2.949	0.553	-0.003	3.6	30.05	29.84	29.57	61.41	1.48	125
13-Jul ²	9:05-11:15	132	53.0	-81.1	1.214	0.251	0.125	32.6	26.69	26.46	25.97	51.09	2.87	354
13-Jul ³	11:35-14:30	58.6	51.8	-7.3	1.031	0.206	-0.178	8.0	27.66	29.37	26.91	44.34	3.34	298
16-Jul ²	9:00-11:15	189	7.97	-181	1.952	0.386	-0.064	0	28.43	30.67	26.35	64.79	1.04	81
16-Jul ³	11:35-14:30	144	24.0	-120	1.741	0.347	-0.093	0	30.40	31.62	28.11	56.67	1.03	72
18-Jul ¹	5:30-8:20	53.4	29.7	-23.1	1.132	0.216	-0.047	100	21.15	22.37	24.94	93.05	2.18	429
18-Jul ³	8:40-11:40	558	-11.0	-569	1.555	0.318	-0.231	NA	28.16	NA	27.07	71.25	2.24	229
20-Jul ²	7:00-10:00	111	1.93	-109	1.556	0.274	-0.126	2	28.00	NA	25.95	64.03	2.26	235
27-Jul ¹	1:05-4:42	9.48	-4.18	-14.3	0.342	0.035	0.611	53	20.85	20.08	25.90	89.71	1.53	393
27-Jul ¹	5:01-9:05	58.0	0.43	-57.6	0.221	0.043	0.98	14	23.77	24.29	25.21	78.42	2.39	377
1-Aug ²	8:35-11:45	122	33.8	-87	1.262	0.246	-0.62	0	30.68	34.21	26.76	56.61	2.81	148
1-Aug ³	12:10-15:04	101	33.8	-68.5	1.725	0.307	-0.277	0	33.60	37.28	29.61	40.29	1.08	41

* Positive and negative fluxes are defined as net emissions and depositions respectively. ^{1,2,3} Profile categories 1, 2 and 3 from the text respectively.

List of Figures

Figure 1. Comparison between measured and modeled normalized mean wind speed and momentum flux profiles. The data are from Wilson (47) (black circles) and K- ϵ model (black line) and the analytical model (dashed gray line) estimates of the mean wind speed normalized by u_* (a) and the Reynolds's stress normalized by u_*^2 are plotted as a function of height normalized by canopy height (b).

Figure 2. Scatter plot of measured and integrated modeled kinematic sensible heat fluxes, $\overline{w'T'}$ at the canopy top (black circles) and in the canopy (grey triangles, $z/h_c = 0.23$ to 0.68) (a). Hourly averages of eddy covariance (dotted line) and closure model (dashed lines) sensible heat fluxes are shown. The shaded area represents \pm one standard deviation bounds from the eddy covariance flux measurements (b).

Figure 3. Measured NH_3 concentration profiles from July 6th to August 1st for in-canopy sampling periods before (a), during (b), after (c) the time frame of the average morning concentration peak. The lines indicate smoothed concentration profiles needed in first and second derivative estimations when determining the source/sink profile (S).

Figure 4. Above canopy modified Bowen ratio NH_3 (AMANDA MBR) flux vs. the NH_3 flux derived from integrating the analytical closure model (ACM) source sink profile, S , to the canopy top (Integrated in-canopy).

Figure 5. Box plots and mean (grey bar) and whiskers represent the 5th and 95th percentile of the dimensionless diurnal NH_3 concentration normalized by the average daily concentration, $z = 1\text{m}$ (top panel) and above-canopy MBR NH_3 flux estimates. Positive values indicate emissions and negative values indicate deposition (bottom panel) from July 6th through August 1st. The notches are the

1 asymptotic normality of the median and represent the 95% confidence interval for the difference in
2 two medians.

3

4

5

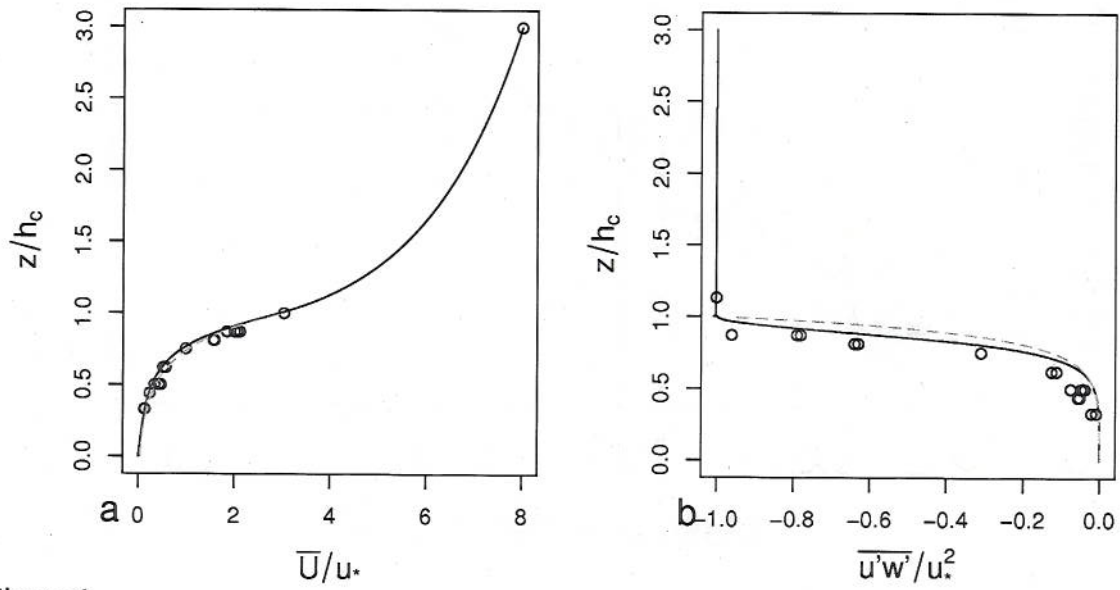
1 Table of Contents Brief:

2

3 The development and evaluation of an analytical first order closure model to estimate in-
4 canopy sources and sinks of ammonia in fertilized *Zea mays* field

5

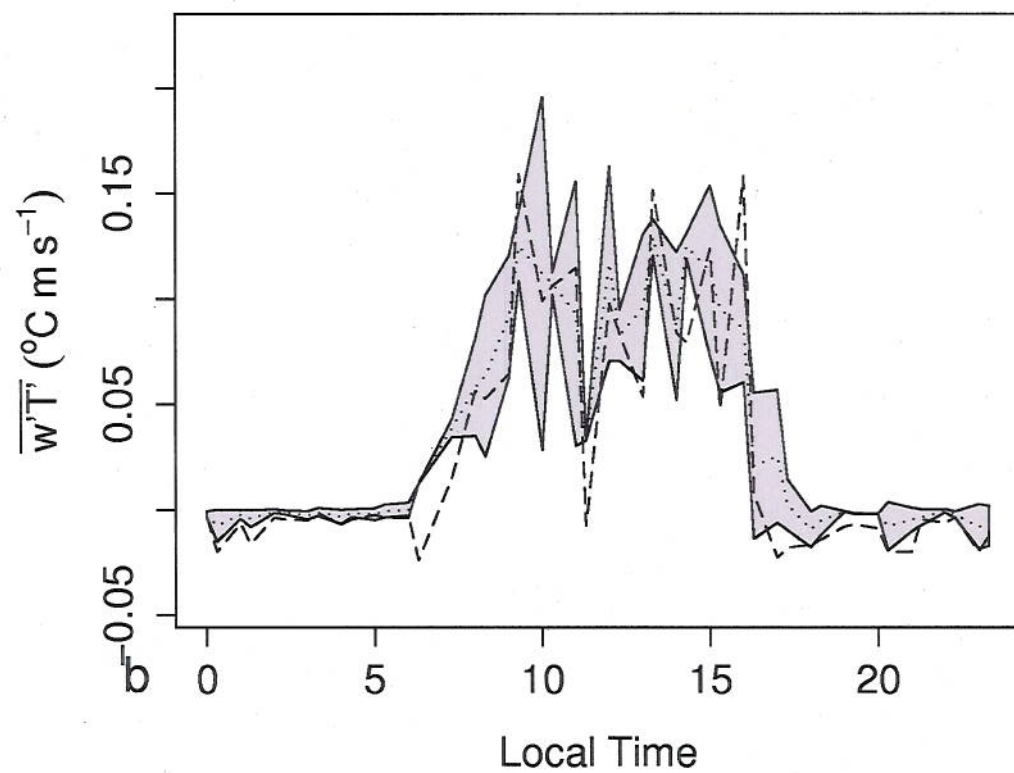
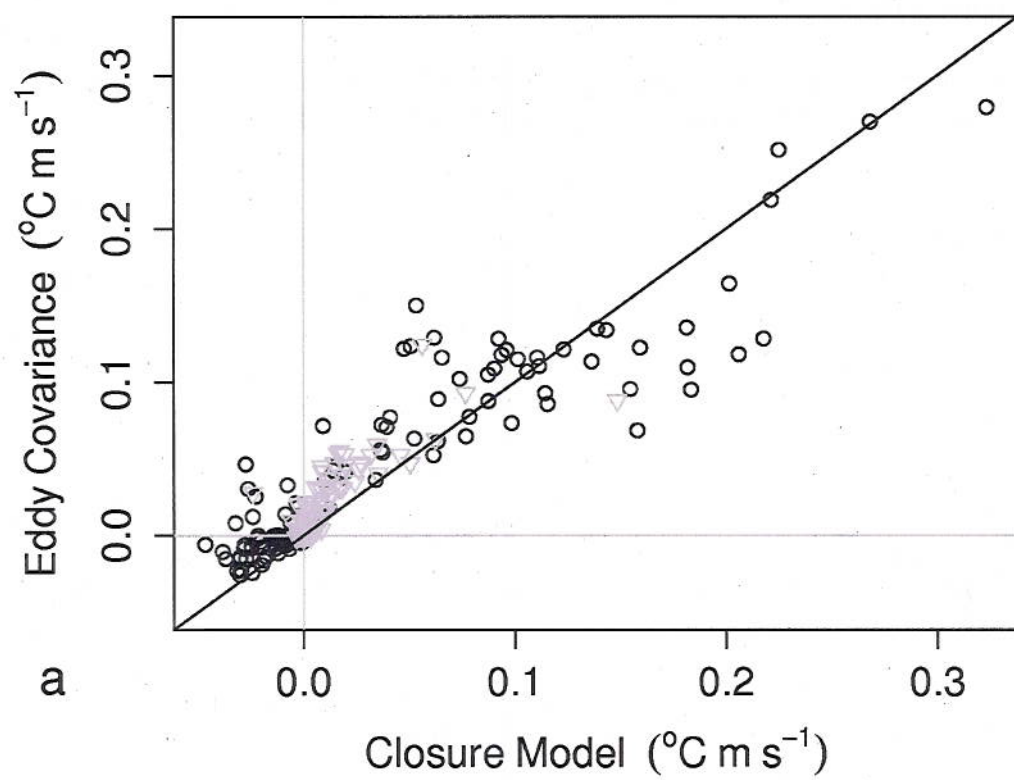
6



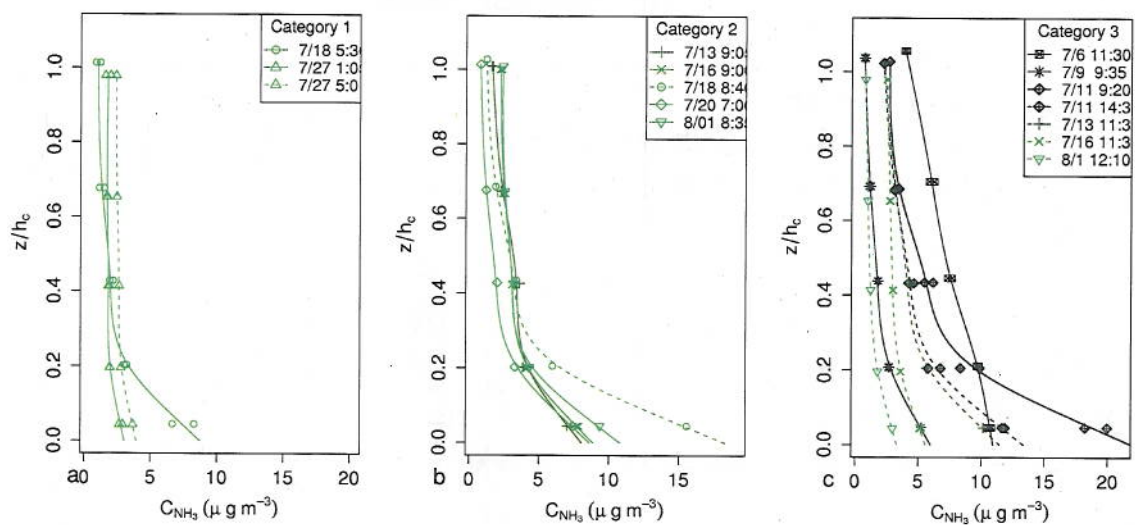
7

8

Figure 1.

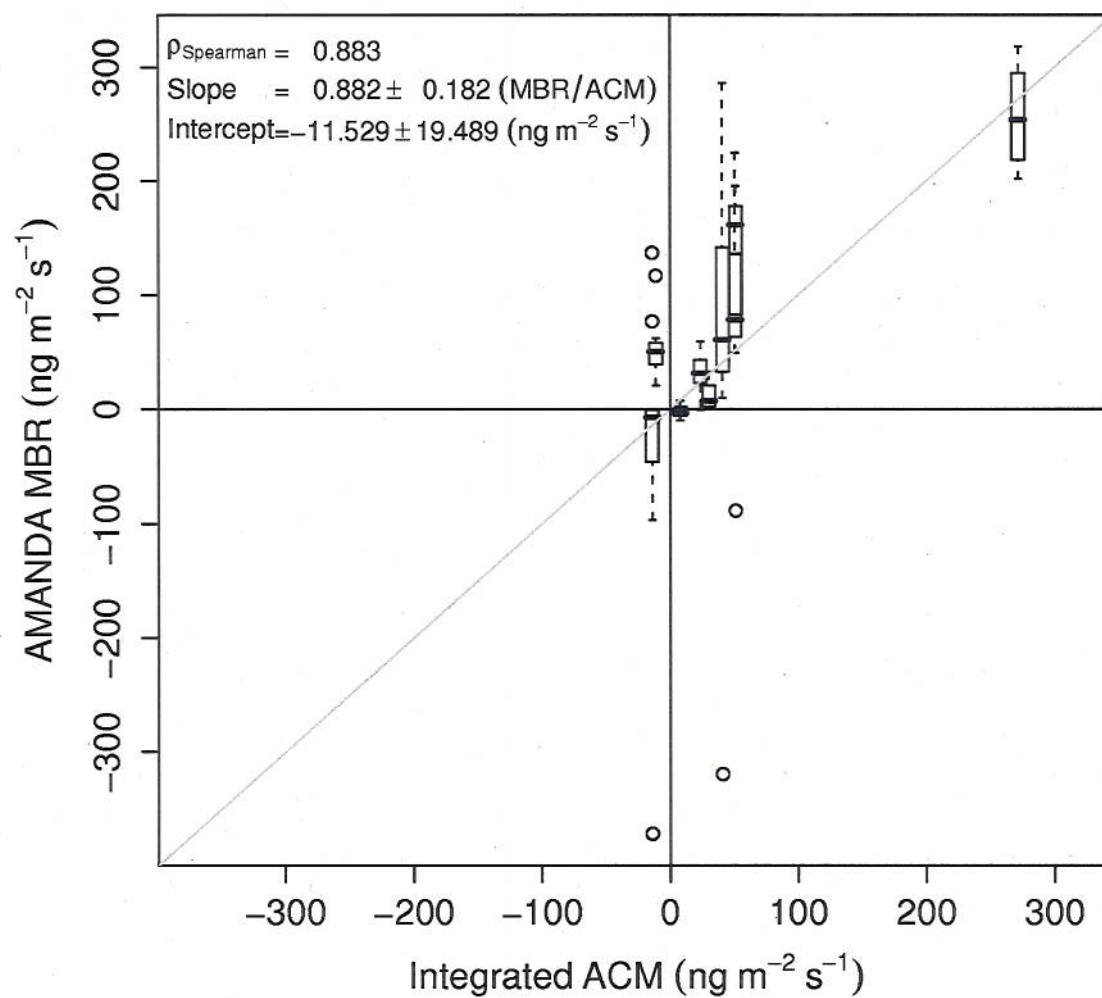


1
2 Figure 2.

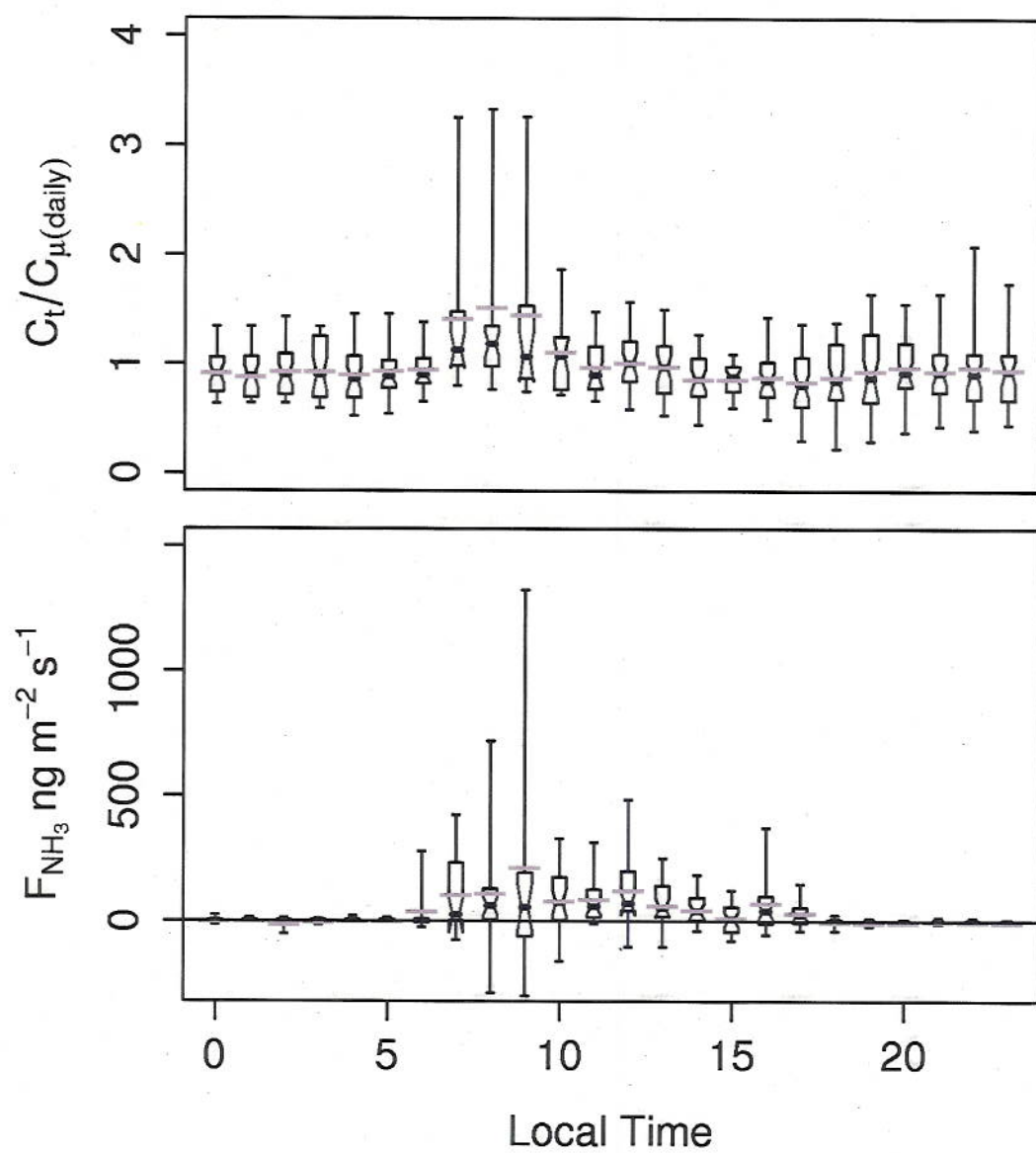


1
2 Figure 3.

NH₃ flux estimates



1
2 Figure 4.



1
2 Figure 5.

1 Estimation of in-canopy ammonia sources and sinks in a fertilized

2 *Zea mays* field

3
4 Jesse O. Bash, John T. Walker, Gabriel G. Katul, Matthew R. Jones, Eiko Nemitz,

5 Wayne P. Robarge

6 7 8 Table of contents

9		
10	Text S1: Application of first order closure approximation to ammonia in fertilized	
11	agricultural settings	S2
12	Figure S1: model residuals vs. gradient strength	S5
13	Text S2: In-canopy mean air-temperature profiles	S5
14	Figure S2: In-canopy temperature profiles	S7
15	Figure S3: In-canopy sensible heat flux profiles	S8
16	Text S3: In-canopy NH ₃ flux profiles	S8
17	Figure S4: In-canopy ammonia source/sink and flux profiles	S10
18	Figure S5: In-canopy ammonia concentration change with respect to time	S12
19		

Supplementary Material

Text S1. Applicability of first order closure approximations to ammonia in fertilized agricultural settings

While first-order closure models may be questionable on theoretical grounds for canopy flows, there may be a justification for their usage in the case of ammonia in fertilized agricultural settings. To illustrate, consider a stationary and planar-homogeneous high Reynolds number and Peclet number flow so that the one-dimensional budget equation for an arbitrary turbulent scalar ($=\xi$) flux is given by (26)

$$\frac{\partial \langle w' \xi' \rangle}{\partial t} = 0 = \underbrace{-\langle w' w' \rangle \frac{\partial \langle \xi \rangle}{\partial z}}_I - \underbrace{\frac{\partial}{\partial z} \langle w' w' \xi' \rangle}_{II} - \underbrace{\frac{1}{\rho} \langle \xi' \frac{\partial p'}{\partial z} \rangle}_{III} + \underbrace{\frac{g}{\langle T \rangle} \langle T' \xi' \rangle}_{IV}, \quad (S1)$$

where w is the vertical velocity component, p is the atmospheric turbulent pressure, T is the ambient mean air temperature, g is the gravitational acceleration, t is time, and z is the vertical direction ($z=0$ is at the ground). An angular bracket and overbar denote the usual planar and temporal averaging, and primes denote perturbation from the mean. For notational simplicity, the $\langle \cdot \rangle$ was not shown in the main text though it was assumed that all averaging operations are spatial and temporal inside the canopy. The terms on the right hand side of equation S1 are defined as follows: term (I) is the flux production, term (II) is the flux-transport, term (III) is the scalar-pressure interaction (a decorrelation or dissipation term), and term (IV) is the buoyancy production or dissipation term. As is generally the case in higher order closure modeling, this budget requires parameterizations for terms (II) – (IV). If the dissipation term is parameterized as:

$$\frac{1}{\rho} \left\langle \xi' \frac{\partial p'}{\partial z} \right\rangle = C_4 \frac{\langle w' \xi' \rangle}{\tau}, \quad (\text{S2})$$

and the flux transport term is given as (26):

$$\langle w' w' \xi' \rangle = -C_5 \tau \sigma_w^2 \frac{\partial \langle w' \xi' \rangle}{\partial z} = -C_5 \tau \sigma_w^2 S_c \quad (\text{S3})$$

then upon replacing these terms in the flux budget equation and re-arranging, we obtain:

$$\langle w' \xi' \rangle = \frac{\tau}{C_4} \left[-\langle w' w' \rangle \frac{\partial \langle \xi' \rangle}{\partial z} + C_5 \frac{\partial}{\partial z} (\tau \sigma_w^2 S_c) + \frac{g}{\langle T \rangle} \langle T' \xi' \rangle \right], \quad (\text{S4})$$

where τ is a relaxation time scale defined as the ratio of the turbulent kinetic energy to its

mean dissipation rate, σ_w^2 is the variance of the vertical velocity component, and C_4 and

C_5 are closure constants. The formulation in S4 resembles LNF in that the flux-transport

term is now made explicitly dependent on the local source strength (or near-field effects

of vegetation sources and sinks), but also allows for their inhomogeneity (locally,

$\partial S_c / \partial z \neq 0$ here) and accounts for the local effects of thermal stratification. We expect

that when

$$\left| \sigma_w^2 \frac{\partial \langle \xi' \rangle}{\partial z} \right| \gg \left| C_5 \frac{\partial}{\partial z} (\tau \sigma_w^2 S_c) + \frac{g}{\langle T \rangle} \langle T' \xi' \rangle \right|, \quad (\text{S5})$$

the gradient-diffusion (or first order closure) argument holds inside the canopy. For NH_3

in a fertilized setting, $|\partial \langle \xi' \rangle / \partial z|$ is expected to be large (Figure 3). Hence, for these

‘strong-gradient’ situations, a first-order closure model may be appropriate given the

dominance of the production term (term *I*) over the flux-transport term (term *II*). We

should note that the ‘strong-gradient’ assumptions here need hold for other scalars such

as air temperature or water vapor.

The magnitude of the in-canopy gradient relative to the above canopy value ,
referred to here as the normalized gradient, was calculated for air temperature and NH₃
concentration using:

$$\frac{h_c}{\bar{\xi}_{2.25}} \frac{|\Delta \bar{\xi}|}{\Delta z}, \quad (S6)$$

where $\bar{\xi}_{2.25}$ was the average concentration or temperature at 2.25 m, $|\Delta \bar{\xi}|$ was defined as
the absolute value of the maximum measured difference within the canopy, h_c was
defined as the canopy height, and Δz was set 2.15 m, the difference between the highest
and lowest measurement points. The mean normalized gradients for temperature (°C)
and NH₃ (μg m⁻³) were 0.036±0.026 and 4.38±3.21, respectively. The average maximum
temperature difference in the in-canopy profile measurements was 0.98 °C (1.62% of the
ambient above canopy measurement). In contrast, the average maximum NH₃
concentration difference was 6.52 μg m⁻³ (194% of the average above canopy
concentration). The NH₃ concentration profiles do suggest that the “strong gradient”
requirement is plausible. The model performance in estimating sensible heat as a function
of the gradient in maximum range of the temperature profiles is illustrated in Figure S1.
The model sensible heat flux residuals normalized to the measured value are lower for
cases with a larger in-canopy temperature gradient as expected using first order closure
arguments presented here.

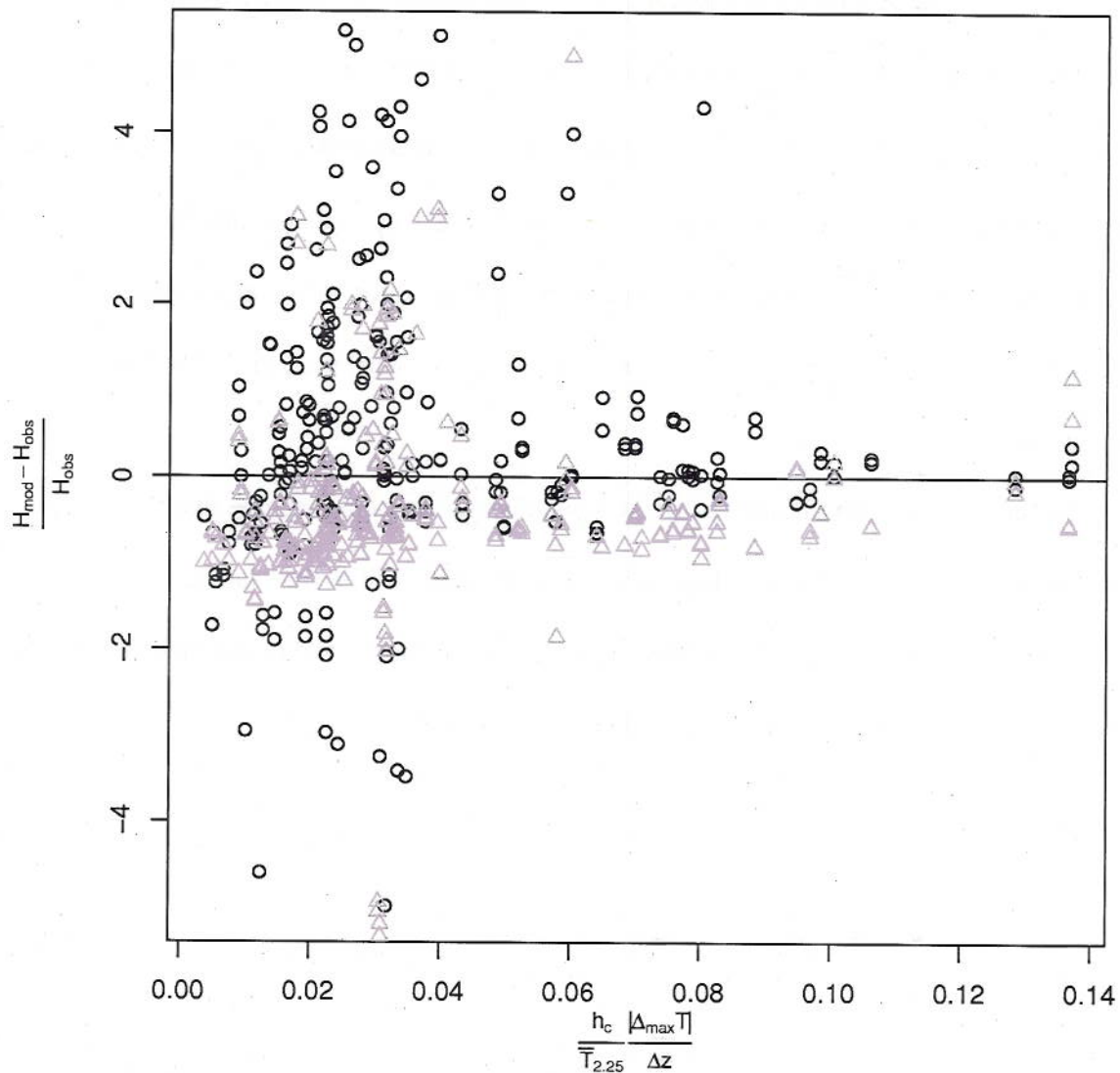


Figure S1, normalized residual of the sensible heat flux as a function of the gradient in the maximum range of the measured temperature profile ($^{\circ}\text{C}$) normalized by the 2.25 meter temperature measurement ($^{\circ}\text{C}$).

Text S2. In-canopy mean air temperature profiles

Mean air temperature profile measurements collocated with the in-canopy NH_3 concentration profiles were made throughout the in-canopy sampling period. Estimation of the in-canopy sensible heat flux using measured mean air temperature profiles can be used to explore the model performance by comparison to in-canopy measured sensible

1 heat fluxes. As earlier noted in equation S5 and the analysis in Figure S1, there is no
2 reason to suspect that the flux-transport term or, more important, the buoyancy term
3 $\sigma_T^2 (g / T)$ to be small. In fact, σ_T^2 , the main culprit in the buoyancy term for heat can be
4 large inside canopies when compared to co-variances between a scalar and air
5 temperature. Hence, this evaluation of model performance for temperature must be
6 viewed as a ‘worst-case’ scenario when extrapolating this performance to NH3 in
7 agricultural settings.

8 First order closure methods applied to the sensible heat flux also assume that the canopy
9 and soil storage of heat is negligible and that the direction of the flux can be inferred
10 from the mean air temperature gradient. Again, these assumptions are not satisfied during
11 periods of rapid heating and cooling of the canopy and soil.

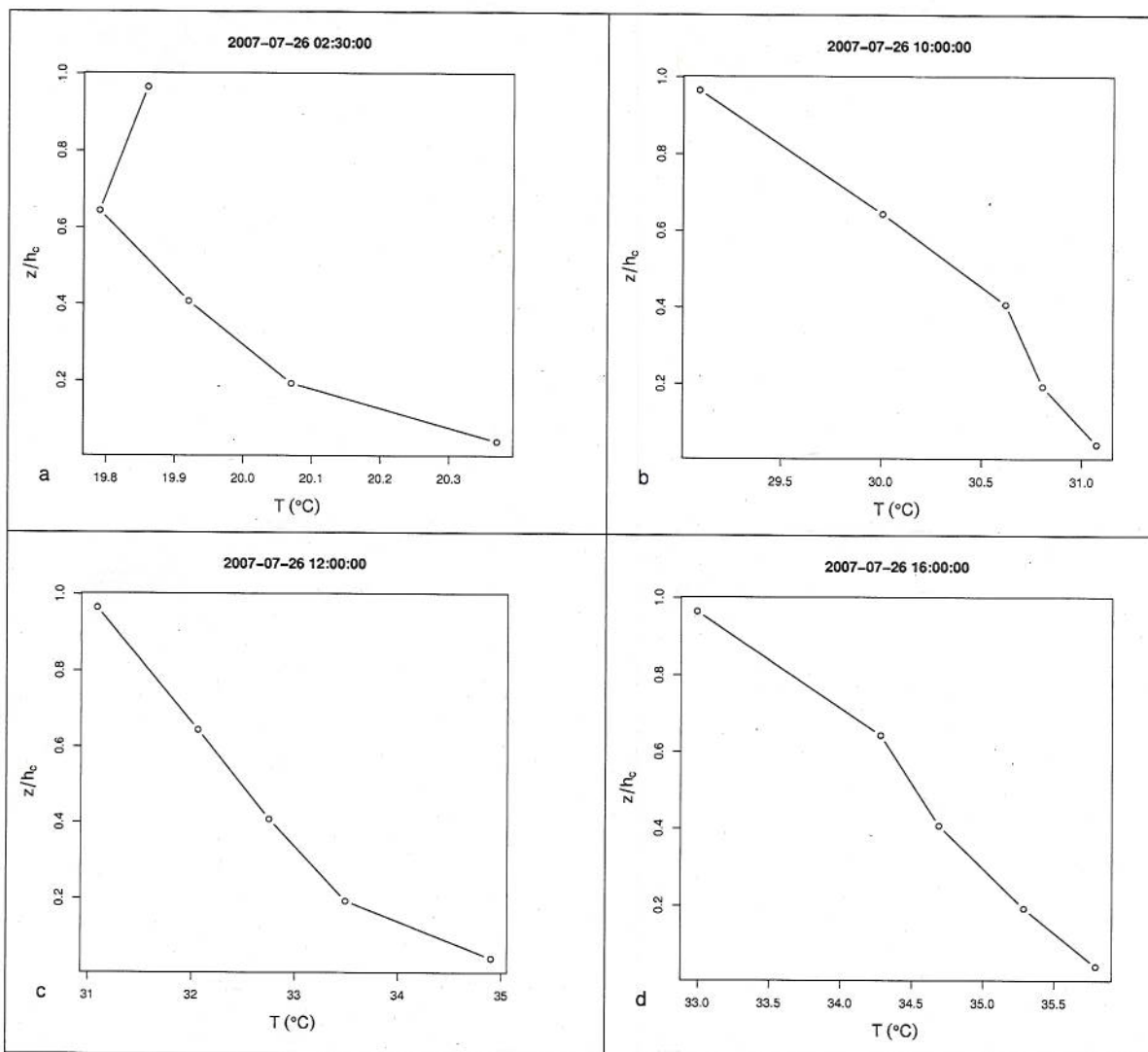


Figure S2, Examples of the in-canopy mean air temperature profiles during a cloud free day measured at 2:30 (a), 10:00 (b), 12:00 (c), and 16:00 (d) local time.

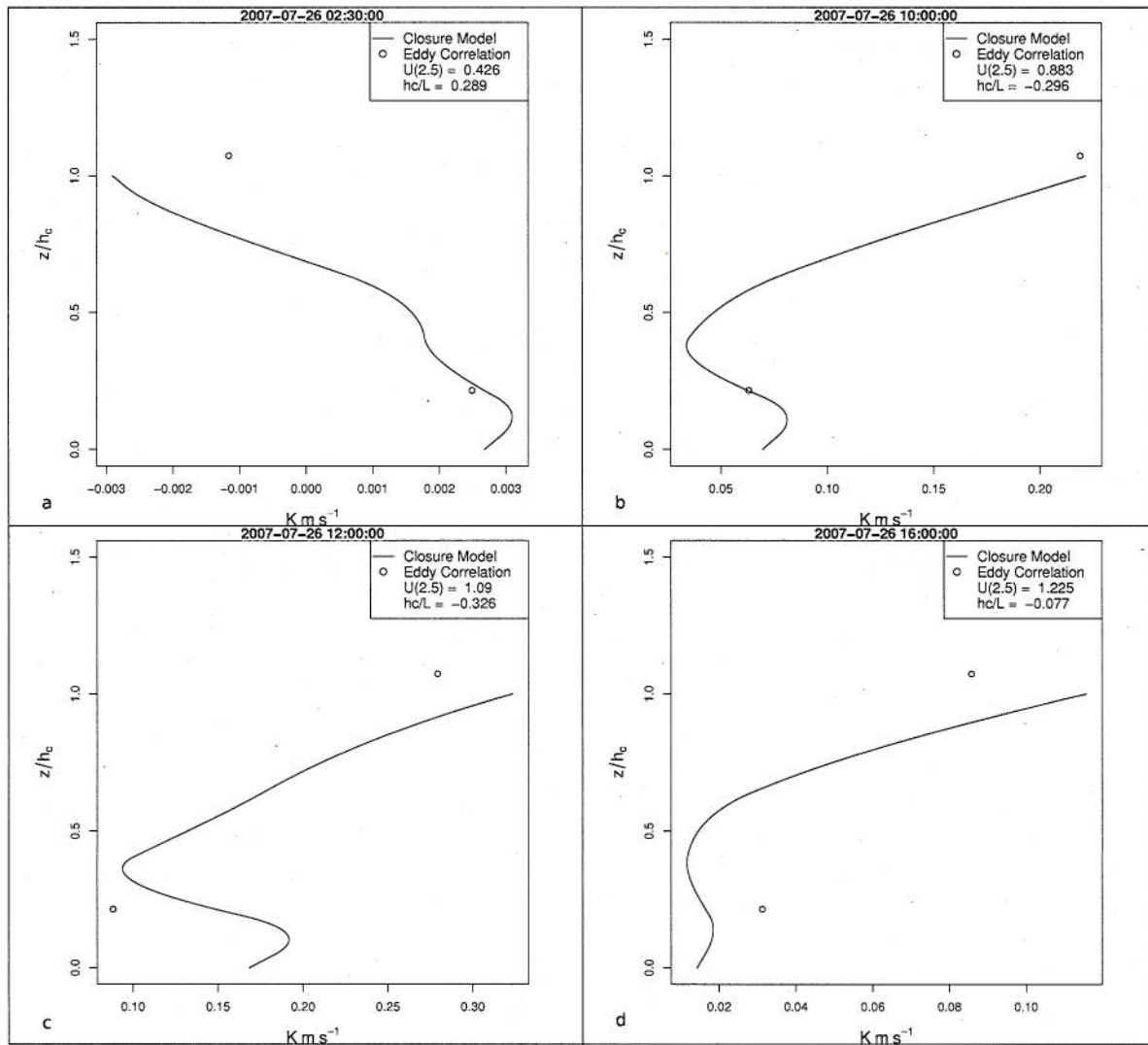


Figure S3, examples of the in-canopy integrated flux profiles during a cloud free day at closure model estimates are shown as the solid line and eddy covariance measurements are shown as a circle for 2:30 (a), 10:00 (b), 12:00, (c), and 16:00 (d) local time

Figure S2 shows example air temperature profiles used in the estimation of the sensible heat flux inside and above the canopy (Figure S3). Notice that the mean air temperature is highest near the ground.

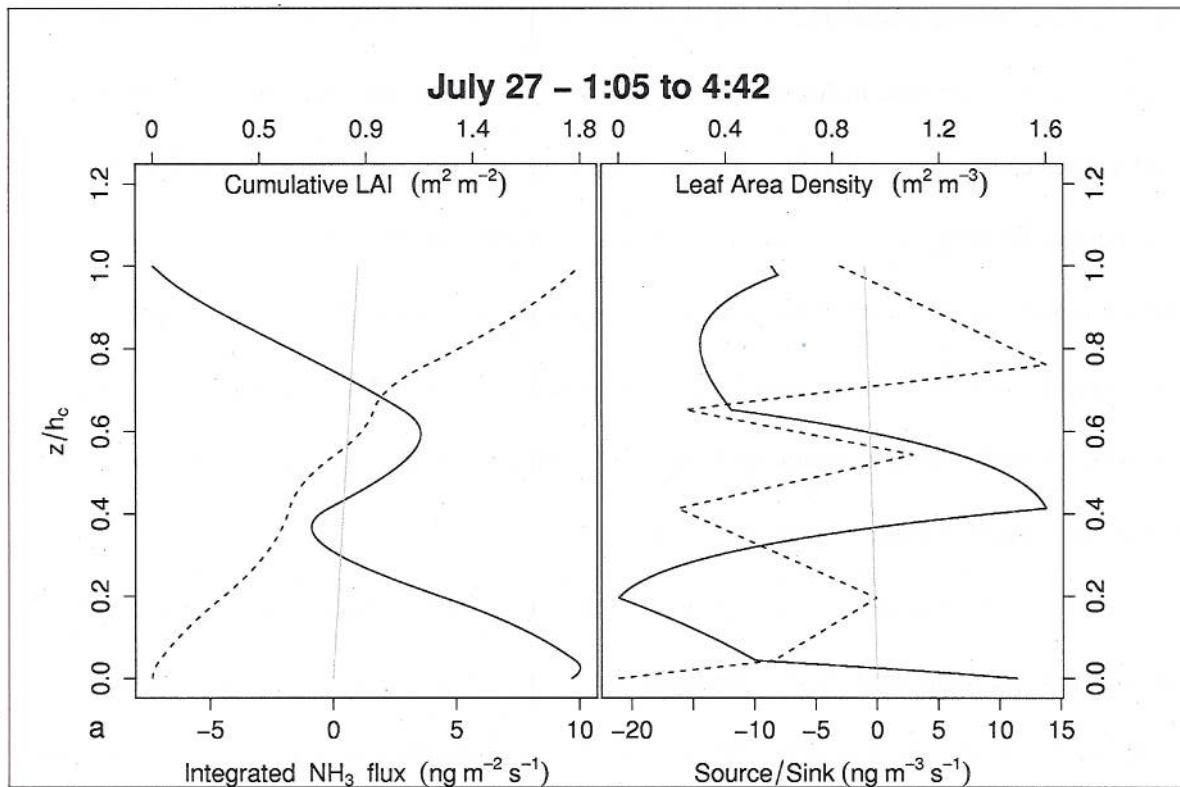
Text S3. In-canopy NH_3 flux profiles

The above-canopy NH_3 concentration increased from the early morning to a daily maximum at approximately 9:30 EST. In-canopy NH_3 mean concentration

1 measurements comprised six back to back sampling events leading up to and following
2 the daily peak indicate that the in-canopy concentrations follow this diel pattern. The
3 largest increases in the in-canopy concentrations were measured at 0.1m (the lowest
4 sampling height). In-canopy closure model estimates of the flux indicate that this
5 concentration increase was due to evasion of NH_3 from the fertilized soil surface, Figure
6 S4. The modeled source sink profiles suggest that the majority of the NH_3 emitted at the
7 soil surface is then recaptured by the canopy, Figure S4. Given the fact that the leaf area
8 density was never used in the mean scalar concentration budget, the agreement between
9 the shapes of the sink strength and the leaf area density profile is rather remarkable,
10 further confirming the role of foliage uptake, especially for the July 13th. This
11 relationship was not seen in the source sink profiles estimated for the stable nighttime
12 measurements when the stoma would be expected to be closed on July 27th indicating the
13 possibility of different stomatal and cuticular uptake rates and mechanisms in agreement
14 with the proposed models of Sutton *et al.* (10).

15 To further explore the observed morning peak in above-canopy concentrations
16 and fluxes, we examined the temporal pattern of in-canopy concentrations measured
17 between 1:00 AM and 2:30 PM EST (Figure S5). To illustrate relative changes over time,
18 concentrations within sequential sampling events ($N = 6$) were normalized by the
19 concentration measurement of the first set of samples. Intercepts of a linear regression of
20 fractional changes in the in-canopy ambient concentration versus the midpoint in
21 sampling when denuders were changed are significantly different from zero ($p < 0.001$)
22 with a mean intercept of 9:52 AM EST for all sample heights and range from 10:15 AM
23 EST at 0.1 m to 9:28 AM EST at 0.95 m. Slopes were significant at $p < 0.05$ for all

1 denuder sampling heights with a mean value of $-1.235 \% h^{-2}$ and ranged from -1.024 at z
 2 $= 0.1$ to -1.594 at $z = 2.25$. The delay in the reduction of the in-canopy NH_3
 3 concentration following the peak in the above-canopy concentrations can be partially
 4 explained by the storage flux term in the canopy, the temperature/chemical partitioning of
 5 NH_3 on vegetation and soil and/or the rapid growth of the planetary boundary layer in the
 6 morning that can introduce a finite \bar{w} (these were not considered in the model).



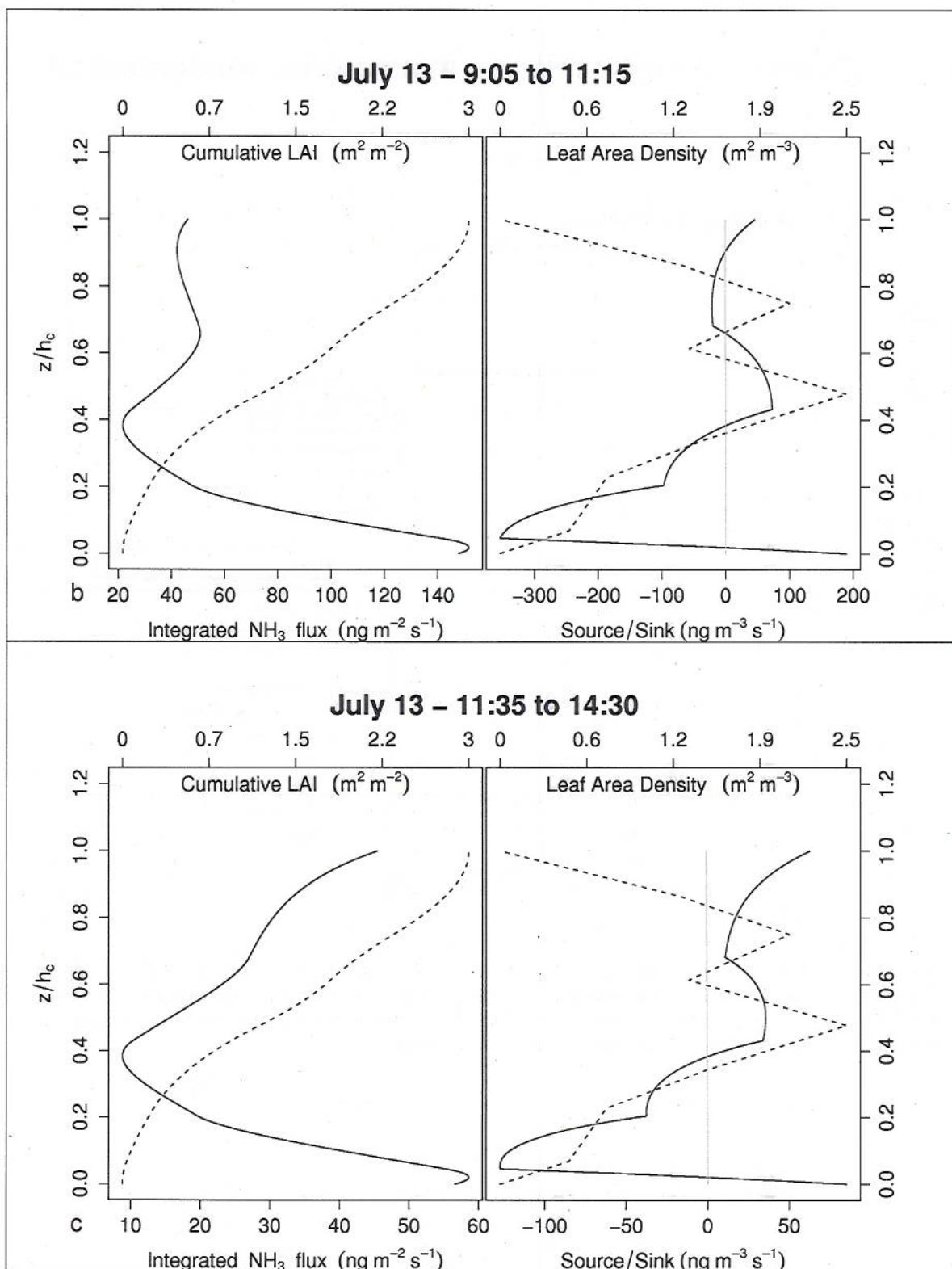


Figure S4, Examples of turbulent flux and mean NH_3 source-sink profiles (solid lines) and measured leaf area density and cumulative LAI profiles (dotted lines) during the early morning (a) mid morning (b) and afternoon (c).

Canopy sublayer change in ammonia concentrations

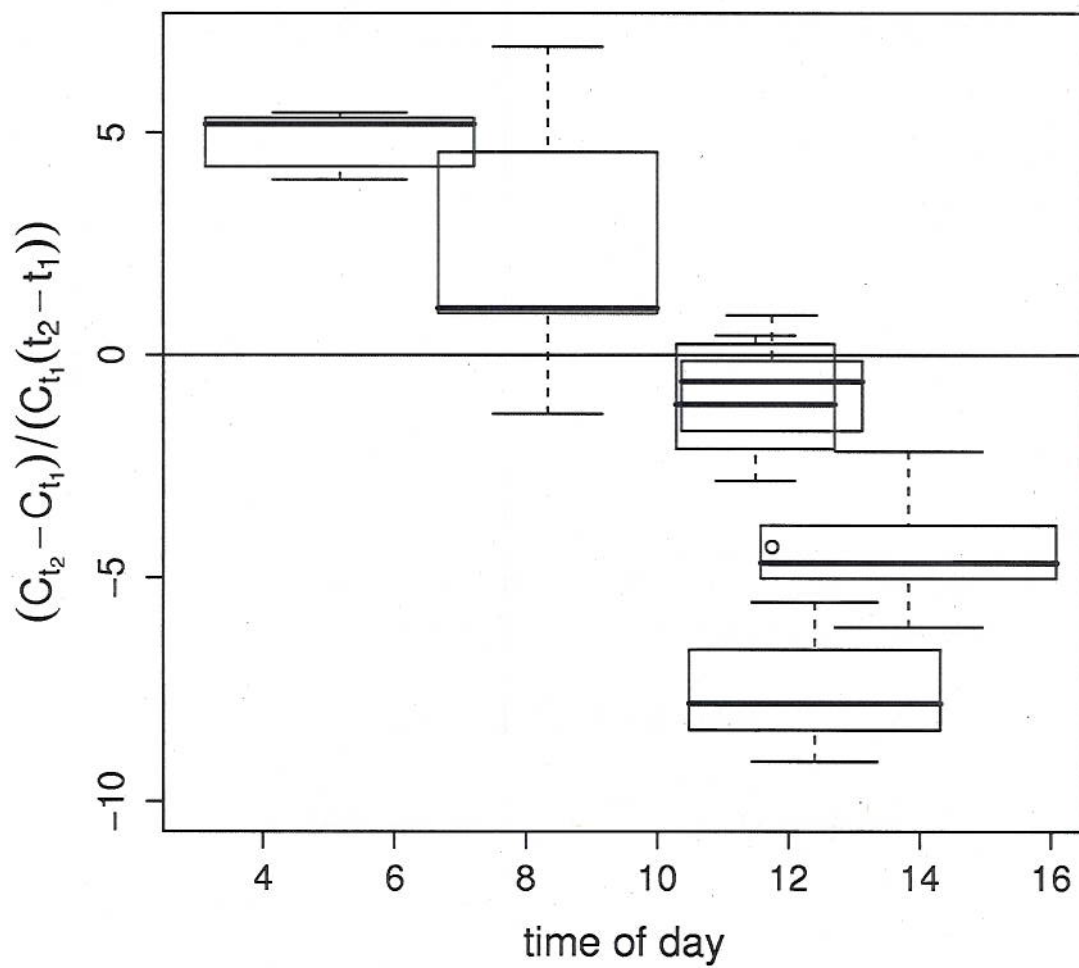


Figure S5. Box plots of the change in ambient concentrations relative to the first set of measurements with respect to time. Positive values indicate an increase and negative values indicate a decrease in the in-canopy mean NH_3 concentration. The widths of the box plots are proportional to the sum of the sampling times used to estimate the concentration changes.